

Light baryons and their electromagnetic interactions in the covariant constituent quark model

Thomas Gutsche,¹ Mikhail A. Ivanov,² Jürgen G. Körner,³ Valery E. Lyubovitskij ^{*,1} and Pietro Santorelli⁴

¹*Institut für Theoretische Physik, Universität Tübingen,
Kepler Center for Astro and Particle Physics,
Auf der Morgenstelle 14, D-72076, Tübingen, Germany*

²*Bogoliubov Laboratory of Theoretical Physics,
Joint Institute for Nuclear Research, 141980 Dubna, Russia*

³*Institut für Physik, Johannes Gutenberg-Universität,
D-55099 Mainz, Germany*

⁴*Dipartimento di Scienze Fisiche, Università di Napoli Federico II,
Complesso Universitario di Monte S. Angelo, Via Cintia, Edificio 6,
80126 Napoli, Italy, and Istituto Nazionale di Fisica Nucleare, Sezione di Napoli*

We extend the confined covariant constituent quark model that was previously developed by us for mesons to the baryon sector. In our numerical calculation we use the same values for the constituent quark masses and the infrared cutoff as have been previously used in the meson sector. In a first application we describe the static properties of the proton and neutron, and the Λ -hyperon (magnetic moments and charge radii) and the behavior of the nucleon form factors at low momentum transfers. We discuss in some detail the conservation of gauge invariance of the electromagnetic transition matrix elements in the presence of a nonlocal coupling of the baryons to the three constituent quark fields.

PACS numbers: 12.39.Ki,13.20.He,14.20.Jn,14.20.Mr

Keywords: relativistic quark model, confinement, light and bottom baryons, electromagnetic form factors

I. INTRODUCTION

We use the confined covariant constituent quark model (for short: covariant quark model) as dynamical input to calculate the electromagnetic transition matrix elements between light (u, d, s) baryons. In the covariant quark model the current-induced transitions between baryons are calculated from two-loop Feynman diagrams with free quark propagators in which the high energy behavior of the loop integrations is tempered by Gaussian vertex functions [1–4]. An attractive new feature has recently been added to the covariant quark model inasmuch as quark confinement has now been incorporated in an effective way, i.e. there are no quark thresholds and thus no free quarks in the relevant Feynman diagrams [5, 6]. We emphasize that the covariant quark model described here is a truly frame-independent field theoretical quark model in contrast to other constituent quark models which are basically quantum mechanical with built-in relativistic elements.

In the covariant quark model we use the same values for the constituent quark masses and the infrared cutoff for all hadrons (mesons and baryons) independent of the hadron masses. We believe that the formulation of the confined covariant quark model constitutes a major advance both from the conceptual and the practical point of view. While an unconfined quark model is valid only for hadrons with masses low enough to lie below the sum of the constituent quark masses the confined covariant quark model can be applied to all hadrons regardless of their masses. The viability of the improved covariant quark model was demonstrated in a number of applications to mesonic transitions in [5]. The form factors of the $B(B_s) \rightarrow P(V)$ transitions were evaluated in [6], in a parameter-free way, in the full kinematical region of momentum transfer. As an application, the widths of some nonleptonic B_s decays were also calculated. This approach was successfully applied to a study of the tetraquark state $X(3872)$ and its strong and radiative decays (see, Refs. [7, 8]).

In the present paper we formulate the covariant quark model with infrared confinement for the baryon sector. By keeping the same values for the constituent quark masses and the infrared cutoff as had been used in the meson sector we are able to reduce the number of free model parameters in the baryon sector to essentially the set of baryon size parameters. As a first application we describe the static properties of the nucleon and the Λ -baryon (magnetic moments and charge radii) and the behavior of the nucleon form factors at low momentum transfer. In a forthcoming

* On leave of absence from Department of Physics, Tomsk State University, 634050 Tomsk, Russia

publication [9] we are planning to study the rare decays of the Λ_b -baryon into the Λ_s or the neutron. The present paper provides the necessary input for such a calculation in as much we determine the properties of the light baryons from their electromagnetic interactions.

The paper is structured as follows. In Sec. II we review the basic notions of our dynamical approach — *the covariant quark model for baryons*. We present the interaction Lagrangian describing the nonlocal coupling of a proton to its constituents, discuss the choice of interpolating currents and the vertex function, recall the compositeness condition for bound-state hadrons and show how the confinement ansatz is implemented in the baryon sector. In Sec. III we include the electromagnetic interactions of quarks and charged baryons in a manifestly gauge-invariant way, derive the Lagrangian describing the nonlocal interaction of the baryon, quark and electromagnetic fields. In Sec. IV we present the loop integration techniques that allow one to calculate the nucleon mass function and its derivative and the electromagnetic form factors of the nucleons. By analytically verifying the pertinent Ward and Ward–Takahashi identities we discuss in some detail how gauge invariance is maintained in the electromagnetic transitions. Sec. IV also contains our numerical results for the magnetic moments and form factors of the proton and neutron. We find that a particular superposition of vector and tensor interpolating currents gives satisfactory results for the nucleon static properties and form factors at low energies. In Sec. V we extend our approach to describe the static properties of the Λ_s hyperon. We summarize our findings in Sec. VI.

II. THE COVARIANT QUARK MODEL FOR BARYONS

The basic ingredients of the covariant quark model for baryonic three quark states prior to the implementation of confinement can be found in [1–4]. This includes a description of the structure of the Gaussian vertex factor, the choice of interpolating baryon currents as well as the compositeness condition for baryons.

The new features introduced to the meson sector in [5, 6] and applied to the baryon sector in this paper are both technical and conceptual. Instead of using Feynman parameters for the evaluation of the two-loop baryonic quark model Feynman diagram we now use Schwinger parameters. The technical advantage is that this leads to a simplification of the tensor loop integrations inasmuch as the loop momenta occurring in the quark propagators can be written as derivative operators. Furthermore, the use of Schwinger parameters allows one to incorporate quark confinement in an effective way. Details of these two new features of the covariant quark model have been described in [5, 6].

Let us enumerate the number of model parameters that are needed in our approach for the description of baryons. As stated in the introduction the values of the constituent quark masses and the universal confinement parameter are taken over from the meson sector. The coupling strength of a baryon to its constituent quarks is fixed by the compositeness condition. This leaves one with one size parameter for each baryon. For the present paper we need the size parameters of the proton, neutron and Λ_s . Naturally we use the same size parameter for the proton and the neutron. The size parameters are determined by a fit to the static e.m. properties and form factors of the nucleons and the Λ_s . We have added one more parameter to the set of basic parameters which describes the mixing between vector and tensor interpolating currents.

A. Lagrangian and three-quark currents

Let us begin our discussion with the proton. The coupling of a proton to its constituent quarks is described by the Lagrangian

$$\mathcal{L}_{\text{int}}^p(x) = g_N \bar{p}(x) \cdot J_p(x) + g_N \bar{J}_p(x) \cdot p(x), \quad (1)$$

where we make use of the same interpolating three-quark current $J_p(\bar{J}_p)$ as in Ref. [11]

$$\begin{aligned} J_p(x) &= \int dx_1 \int dx_2 \int dx_3 F_N(x; x_1, x_2, x_3) J_{3q}^{(p)}(x_1, x_2, x_3), \\ J_{3q}^{(p)}(x_1, x_2, x_3) &= \Gamma^A \gamma^5 d^{a_1}(x_1) \cdot [\epsilon^{a_1 a_2 a_3} u^{a_2}(x_2) C \Gamma_A u^{a_3}(x_3)], \end{aligned} \quad (2)$$

$$\begin{aligned} \bar{J}_p(x) &= \int dx_1 \int dx_2 \int dx_3 F_N(x; x_1, x_2, x_3) \bar{J}_{3q}^{(p)}(x_1, x_2, x_3), \\ \bar{J}_{3q}^{(p)}(x_1, x_2, x_3) &= [\epsilon^{a_1 a_2 a_3} \bar{u}^{a_3}(x_3) \Gamma_A C \bar{u}^{a_2}(x_2)] \cdot \bar{d}^{a_1}(x_1) \gamma^5 \Gamma^A. \end{aligned}$$

The matrix $C = \gamma^0 \gamma^2$ is the usual charge conjugation matrix and the a_i ($i = 1, 2, 3$) are color indices. There are two possible kinds of nonderivative three-quark currents: $\Gamma^A \otimes \Gamma_A = \gamma^\alpha \otimes \gamma_\alpha$ (vector current) and $\Gamma^A \otimes \Gamma_A = \frac{1}{2} \sigma^{\alpha\beta} \otimes \sigma_{\alpha\beta}$ (tensor current) with $\sigma^{\alpha\beta} = \frac{i}{2} (\gamma^\alpha \gamma^\beta - \gamma^\beta \gamma^\alpha)$. The interpolating current of the neutron and the corresponding Lagrangian are obtained from the proton case via $p \rightarrow n$ and $u \leftrightarrow d$. As will become apparent later on, one has to consider a general linear superposition of the vector and tensor currents according to

$$J_N = x J_N^T + (1-x) J_N^V, \quad N = p, n \quad (3)$$

where the mixing parameter x extends from zero to one ($0 \leq x \leq 1$). When taking the nonrelativistic limit of the vector and tensor currents one finds that the two currents become degenerate. The limiting currents for the proton and the neutron read

$$J_p^T \equiv J_p^V = \epsilon^{a_1 a_2 a_3} \vec{\sigma} \psi_d^{a_1} (\psi_u^{a_2} \sigma_2 \vec{\sigma} \psi_u^{a_3}), \quad J_n^T \equiv J_n^V = \epsilon^{a_1 a_2 a_3} \vec{\sigma} \psi_u^{a_1} (\psi_d^{a_2} \sigma_2 \vec{\sigma} \psi_d^{a_3}), \quad (4)$$

where $\psi_{u,d}$ are the upper components of the respective Dirac quark spinor fields and where σ_i are Pauli spin matrices.

Most of the properties of the nucleons are only weakly dependent on the choice of interpolating currents. However, in order to get the correct value for the charge radius of the neutron, one needs to use the superposition of currents Eq. (3) even though the currents J^T and J^V become degenerate in the nonrelativistic limit. In view of the fact that a nonrelativistic description of the neutron gives zero values for the charge radius of the neutron [10] this is an indication that relativistic corrections play a crucial role for the description of the neutron charge radius.

The vertex function F_N characterizes the finite size of the nucleon. We assume that the vertex function is real and the same for the proton and the neutron. To satisfy translational invariance the function F_N has to satisfy the identity

$$F_N(x+a; x_1+a, x_2+a, x_3+a) = F_N(x; x_1, x_2, x_3) \quad (5)$$

for any given 4-vector a . We use the following representation for the vertex function

$$F_N(x; x_1, x_2, x_3) = \delta^{(4)}(x - \sum_{i=1}^3 w_i x_i) \Phi_N \left(\sum_{i<j} (x_i - x_j)^2 \right), \quad (6)$$

where Φ_N is the correlation function of the three constituent quarks with the coordinates x_1, x_2, x_3 and masses m_1, m_2, m_3 , respectively. The variable w_i is defined by $w_i = m_i / (m_1 + m_2 + m_3)$ such that $\sum_{i=1}^3 w_i = 1$. Note that $F_N(x; x_1, x_2, x_3)$ is symmetric in the coordinates x_i , i.e. symmetric under $x_i \leftrightarrow x_j$.

We shall make use of the Jacobi coordinates $\rho_{1,2}$ and the CM coordinate x which are defined by

$$\begin{aligned} x_1 &= x + \frac{1}{\sqrt{2}} w_3 \rho_1 - \frac{1}{\sqrt{6}} (2w_2 + w_3) \rho_2, \\ x_2 &= x + \frac{1}{\sqrt{2}} w_3 \rho_1 + \frac{1}{\sqrt{6}} (2w_1 + w_3) \rho_2, \\ x_3 &= x - \frac{1}{\sqrt{2}} (w_1 + w_2) \rho_1 + \frac{1}{\sqrt{6}} (w_1 - w_2) \rho_2. \end{aligned} \quad (7)$$

The CM coordinate is given by $x = \sum_{i=1}^3 w_i x_i$. In terms of the Jacobi coordinates one obtains

$$\sum_{i<j} (x_i - x_j)^2 = \rho_1^2 + \rho_2^2. \quad (8)$$

Note that the choice of Jacobi coordinates is not unique. With the above choice Eq. (7) one readily arrives at the following representation for the correlation function Φ_N in Eq. (6)

$$\begin{aligned} \Phi_N \left(\sum_{i<j} (x_i - x_j)^2 \right) &= \int \frac{d^4 p_1}{(2\pi)^4} \int \frac{d^4 p_2}{(2\pi)^4} e^{-ip_1(x_1-x_3) - ip_2(x_2-x_3)} \bar{\Phi}_N(-P_1^2 - P_2^2), \\ \bar{\Phi}_N(-P_1^2 - P_2^2) &= \frac{1}{9} \int d^4 \rho_1 \int d^4 \rho_2 e^{iP_1 \rho_1 + iP_2 \rho_2} \Phi_N(\rho_1^2 + \rho_2^2), \\ P_1 &= \frac{1}{\sqrt{2}}(p_1 + p_2), \quad P_2 = -\frac{1}{\sqrt{6}}(p_1 - p_2). \end{aligned} \quad (9)$$

Even if the above choice of Jacobi coordinates was used to derive (9) the representation (9) in its general form can be seen to be valid for any choice of Jacobi coordinates. The particular choice (7) is a preferred choice since it leads

to the specific form of the argument $-P_1^2 - P_2^2 = -\frac{2}{3}(p_1^2 + p_2^2 + p_1 p_2)$. Since this expression is invariant under the transformations: $p_1 \leftrightarrow p_2$, $p_2 \rightarrow -p_2 - p_1$ and $p_1 \rightarrow -p_1 - p_2$, the r.h.s. in Eq. (9) is invariant under permutations of all x_i as it should be.

In the next step we have to specify the function $\bar{\Phi}_N(-P_1^2 - P_2^2) \equiv \bar{\Phi}_N(-P^2)$, which characterizes the finite size of the baryons. We will choose a simple Gaussian form for the function $\bar{\Phi}_N$

$$\bar{\Phi}_N(-P^2) = \exp(P^2/\Lambda_N^2), \quad (10)$$

where Λ_N is a size parameter parametrizing the distribution of quarks inside a nucleon. Note that we have used another definition of the Λ_N in our previous papers: $\Lambda_N = \Lambda_N^{\text{old}}/(3\sqrt{2})$.

Since P^2 turns into $-P_E^2$ in Euclidean space the form (10) has the appropriate fall-off behavior in the Euclidean region. We emphasize that any choice for Φ_N is appropriate as long as it falls off sufficiently fast in the ultraviolet region of Euclidean space to render the corresponding Feynman diagrams ultraviolet finite. The choice of a Gaussian form for Φ_H has obvious calculational advantages.

The coupling constants g_N are determined by the compositeness condition suggested by Weinberg [12] and Salam [13] (for a review, see [14]) and extensively used by us in previous papers on the covariant quark model (for details, see [15]). The compositeness condition postulates that the renormalization constant of the bound-state wave function is set equal to zero. In the case of a baryon this implies that

$$Z_N = 1 - \Sigma'_N(m_N) = 0, \quad (11)$$

where Σ'_N is the on-shell derivative of the nucleon mass function Σ_N , i.e. $\Sigma'_N = \partial \Sigma_N / \partial p$, at $p^2 = m_N^2$ and where m_N is the nucleon mass. The compositeness condition is the central equation of our covariant quark model. It can be viewed as the field theoretic equivalent of the wave function normalization condition for quantum mechanical wave functions. The physical meaning, the implications and corollaries of the compositeness condition have been discussed in some detail in our previous papers (see e.g. [5]).

B. Infrared confinement

In [5] we have shown how the confinement of quarks can be effectively incorporated in the covariant quark model. In a first step, we introduced an additional scale integration in the space of Schwinger's α -parameters with an integration range from zero to infinity. In a second step the scale integration was cut off at the upper limit which corresponds to the introduction of an infrared (IR) cutoff. In this manner all possible thresholds present in the initial quark diagram were removed. The cutoff parameter was taken to be the same for all physical processes. Other model parameters such as the constituent quark masses and size parameters were determined from a fit to experimental data.

Let us describe the basic features of how IR confinement is implemented in our model. All physical matrix elements are described by Feynman diagrams written in terms of a convolution of free quark propagators and the vertex functions. Let n and m be the number of the propagators and vertices, respectively. For the current-induced baryon transitions or the derivative of the mass function one has four quark propagators and two vertex functions, i.e. one has $n = 4$ and $m = 2$. In Minkowski space the two-loop diagram will be represented as

$$\begin{aligned} \Pi(p_1, \dots, p_m) &= \int [d^4 k]^2 \prod_{i_1=1}^m \Phi_{i_1+n}(-K_{i_1+n}^2) \prod_{i_3=1}^n S_{i_3}(\tilde{k}_{i_3} + v_{i_3}), \\ K_{i_1+n}^2 &= \sum_{i_2} (\tilde{k}_{i_1+n}^{(i_2)} + v_{i_1+n}^{(i_2)})^2, \end{aligned} \quad (12)$$

where the vectors \tilde{k}_i are linear combinations of the loop momenta k_i . The v_i are linear combinations of the external momenta p_i . The strings of Dirac matrices appearing in the calculation need not concern us here since they do not depend on the momenta. The external momenta p_i are all chosen to be ingoing such that one has $\sum_{i=1}^m p_i = 0$.

Using the Schwinger representation the local quark propagator is written as

$$S(k) = \frac{1}{m - \not{k}} = (m + \not{k}) \int_0^\infty d\beta e^{-\beta(m^2 - k^2)}. \quad (13)$$

As mentioned before one takes the Gaussian form for the vertex functions, i.e.

$$\bar{\Phi}_{i+n}(-K^2) = \exp[\beta_{i+n} K^2] \quad i = 1, \dots, m, \quad (14)$$

where, as in (10), the parameters β_{i+n} are related to the respective size parameters of the baryons Λ_i via $\beta_{i+n} = 1/\Lambda_i^2$. The integrand in Eq. (12) has a Gaussian form with the exponential factor $(kak+2kr+R)$ where, in case of the baryonic two-loop calculation, a is a 2×2 matrix depending on the parameters β_i , r is a 2-component vector composed from the external momenta, k is a 2-component vector of the loop momenta of the form $k = (k_1, k_2)$ and R is a quadratic form of the external momenta. Tensor loop integrals are calculated with the help of the differential representation

$$k_i^\mu e^{2kr} = \frac{1}{2} \frac{\partial}{\partial r_{i\mu}} e^{2kr}. \quad (15)$$

After doing the loop integration the differential operators $\partial/\partial r_{i\mu}$ will give cause to outer momenta tensors which, in the present case, are p and p' . We have written a FORM [16] program that achieves the necessary commutations of the differential operators in a very efficient way.

After doing the loop integrations one obtains (n denotes the number of propagators)

$$\Pi = \int_0^\infty d^n \beta F(\beta_1, \dots, \beta_n), \quad (16)$$

where F stands for the whole structure of a given diagram. The set of Schwinger parameters β_i can be turned into a simplex by introducing an additional t -integration via the identity

$$1 = \int_0^\infty dt \delta(t - \sum_{i=1}^n \beta_i) \quad (17)$$

leading to

$$\Pi = \int_0^\infty dt t^{n-1} \int_0^1 d^n \alpha \delta\left(1 - \sum_{i=1}^n \alpha_i\right) F(t\alpha_1, \dots, t\alpha_n). \quad (18)$$

There are altogether n numerical integrations: $(n-1)$ α -parameter integrations and the integration over the scale parameter t . The very large t -region corresponds to the region where the singularities of the diagram with its local quark propagators start appearing. However, as described in [5], if one introduces an IR cutoff on the upper limit of the t -integration, all singularities vanish because the integral is now analytic for any value of the set of kinematic variables. We cut off the upper integration at $1/\lambda^2$ and obtain

$$\Pi^c = \int_0^{1/\lambda^2} dt t^{n-1} \int_0^1 d^n \alpha \delta\left(1 - \sum_{i=1}^n \alpha_i\right) F(t\alpha_1, \dots, t\alpha_n). \quad (19)$$

By introducing the IR cutoff one has removed all potential thresholds in the quark loop diagram, i.e. the quarks are never on-shell and are thus effectively confined. We mention that an explicit demonstration of the absence of a two-quark threshold in the case of a scalar one-loop two-point function has been given in Ref. [5]. We take the infrared cutoff parameter λ to be the same in all physical processes. The numerical evaluations have been done by a numerical program written in the FORTRAN code.

III. ELECTROMAGNETIC INTERACTIONS

We use the standard free fermion Lagrangian for the baryon and quark fields:

$$\mathcal{L}_{\text{free}}(x) = \bar{B}(x)(i \not{\partial} - m_B)B(x) + \sum_q \bar{q}(x)(i \not{\partial} - m_q)q(x), \quad (20)$$

where m_q is the constituent quark mass. The interaction with the electromagnetic field has to be introduced both at the baryon and the quark level. In a first step we gauge the free Lagrangians Eq. (20) of the quark and baryon fields in the standard manner by using minimal substitution:

$$\partial^\mu B \rightarrow (\partial^\mu - ie_B A^\mu)B, \quad \partial^\mu q_i \rightarrow (\partial^\mu - ie_{q_i} A^\mu)q_i, \quad (21)$$

where e_B is the electric charge of the baryon B and e_{q_i} is the electric charge of the quark with flavor q_i . The interaction of the baryon and quark fields with the e.m. field is thus specified by minimal substitution. The interaction Lagrangian reads

$$\mathcal{L}_{\text{int}}^{\text{em-min}}(x) = e_B \bar{B}(x) \not{A} B(x) + \sum_q e_q \bar{q}(x) \not{A} q(x). \quad (22)$$

As will become apparent further on, the electromagnetic field does not directly couple to the baryon fields as a result of the compositeness condition.

Next one gauges the nonlocal Lagrangian Eq. (1). The gauging proceeds in a way suggested in Refs. [17, 18] and used before by us (see, for instance, Refs. [11, 19]). In order to guarantee local invariance of the strong interaction Lagrangian one multiplies each quark field $q(x_i)$ in $\mathcal{L}_{\text{int}}^{\text{str}}$ with a gauge field exponential. One then has

$$q_i(x_i) \rightarrow e^{-ie_{q_i} I(x_i, x, P)} q_i(x_i), \quad (23)$$

where

$$I(x_i, x, P) = \int_x^{x_i} dz_\mu A^\mu(z). \quad (24)$$

The path P connects the end-points of the path integral.

It is readily seen that the full Lagrangian is invariant under the transformations

$$\begin{aligned} q_i(x) &\rightarrow e^{ie_{q_i} f(x)} q_i(x), & \bar{q}_i(x) &\rightarrow \bar{q}_i(x) e^{-ie_{q_i} f(x)}, \\ B(x) &\rightarrow e^{ie_B f(x)} B(x), & \bar{B}(x) &\rightarrow \bar{B}(x) e^{-ie_B f(x)}, \\ A^\mu(x) &\rightarrow A^\mu(x) + \partial^\mu f(x), \end{aligned}$$

where $e_B = \sum_{i=1}^3 e_{q_i}$.

One then expands the gauge exponential up to the requisite power of $e_q A_\mu$ needed in the perturbative series. This will give rise to a second term in the nonlocal electromagnetic interaction Lagrangian $\mathcal{L}_{\text{int}}^{\text{em-nonloc}}$. Superficially it appears that the results will depend on the path P taken to connect the end-points in the path integral in Eq. (24). However, one needs to know only the derivatives of the path integral expressions when calculating the perturbative series. Therefore, we use the formalism suggested in [17, 18] which is based on the path-independent definition of the derivative of $I(x, y, P)$:

$$\lim_{dx^\mu \rightarrow 0} dx^\mu \frac{\partial}{\partial x^\mu} I(x, y, P) = \lim_{dx^\mu \rightarrow 0} [I(x + dx, y, P') - I(x, y, P)] \quad (25)$$

where the path P' is obtained from P by shifting the end-point x by dx . The definition (25) leads to the key rule

$$\frac{\partial}{\partial x^\mu} I(x, y, P) = A_\mu(x) \quad (26)$$

which in turn states that the derivative of the path integral $I(x, y, P)$ does not depend on the path P originally used in the definition.

As a result of this rule the Lagrangian describing the nonlocal interaction of the baryon, quark and electromagnetic fields to the first order in the electromagnetic charge reads

$$\mathcal{L}_{\text{int}}^{\text{em-nonloc}}(x) = g_B \bar{B}(x) \cdot \int dy A_\alpha(y) J_{B-\text{em}}^\alpha(x, y) + g_B \int dy A_\alpha(y) \bar{J}_{B-\text{em}}^\alpha(x, y) \cdot B(x), \quad (27)$$

where the nonlocal electromagnetic currents are given by

$$\begin{aligned}
J_{B-\text{em}}^\alpha(x, y) &= \prod_{i=1}^3 \int dx_i J_{3q}^{(B)}(x_1, x_2, x_3) E_B^\alpha(x; x_1, x_2, x_3; y), \\
\bar{J}_{B-\text{em}}^\alpha(x, y) &= \prod_{i=1}^3 \int dx_i \bar{J}_{3q}^{(B)}(x_1, x_2, x_3) E_B^{\alpha\dagger}(x; x_1, x_2, x_3; y), \\
E_B^\alpha(x; x_1, x_2, x_3; y) &= \prod_{i=1}^3 \int \frac{dp_i}{(2\pi)^4} \int \frac{dr}{(2\pi)^4} e^{-i \sum_{i=1}^3 p_i(x-x_i) - ir(x-y)} \tilde{E}_B^\alpha(p_1, p_2, p_3; r), \\
\tilde{E}_B^\alpha(p_1, p_2, p_3; r) &= \sum_{i=1}^3 e_{q_i} \int_0^1 d\tau \left\{ -w_{i1}(w_{i1}r^\alpha + 2q_1^\alpha) \bar{\Phi}'_B(-z_1) - w_{i2}(w_{i2}r^\alpha + 2q_2^\alpha) \bar{\Phi}'_B(-z_2) \right\}, \quad (28)
\end{aligned}$$

Further

$$\begin{aligned}
q_1 &= \sum_{i=1}^3 w_{i1} p_i, & q_2 &= \sum_{i=1}^3 w_{i2} p_i, \\
z_1 &= \tau(w_{i1}r + q_1)^2 - (1-\tau)q_1^2 - (w_{i2}r + q_2)^2, & z_2 &= q_1^2 - \tau(w_{i2}r + q_2)^2 - (1-\tau)q_2^2, \\
w_{i1} &= \begin{pmatrix} \frac{1}{\sqrt{2}}w_3 \\ \frac{1}{\sqrt{2}}w_3 \\ -\frac{1}{\sqrt{2}}(w_1 + w_2) \end{pmatrix}, & w_{i2} &= \begin{pmatrix} -\frac{1}{\sqrt{6}}(2w_2 + w_3) \\ \frac{1}{\sqrt{6}}(2w_1 + w_3) \\ \frac{1}{\sqrt{6}}(w_1 - w_2) \end{pmatrix}. \quad (29)
\end{aligned}$$

IV. NUCLEON MASS FUNCTION AND ELECTROMAGNETIC FORM FACTORS

We start with the calculation of the proton mass function (also called self-energy function) needed for the implementation of the compositeness condition. The relevant term in the expansion of the S -matrix reads

$$\begin{aligned}
S_2 &= i^2 g_N^2 \int dx \int dy \bar{p}(x) \langle 0 | T \{ J_p(x) \bar{J}_p(y) \} | 0 \rangle p(y) \\
&\doteq i \int dx \int dy \bar{p}(x) \Sigma_p(x-y) p(y). \quad (30)
\end{aligned}$$

The corresponding two-loop Feynman quark diagram is shown in Fig. 1. In Eq. (30) we have introduced the standard notation for the proton mass function

$$\Sigma_p(x-y) = i g_N^2 \langle 0 | T \{ J_p(x) \bar{J}_p(y) \} | 0 \rangle. \quad (31)$$

The Fourier-transform of the mass function $\Sigma_p(x-y)$ is given by

$$\Sigma_p(x-y) = \int \frac{d^4 p}{(2\pi)^4} e^{-ip(x-y)} \Sigma_p(p), \quad \Sigma_p(p) = \int d^4 x e^{ipx} \Sigma_p(x). \quad (32)$$

We use the same notation Σ_p for the mass function of the proton in coordinate space and in momentum space. Which of the two representations are being used can be read off from the arguments, *cif.* $\Sigma_p(x-y)$ and $\Sigma_p(p)$. The matrix element of S_2 in Eq. (30) between the initial and final proton states (with momenta p and p' , respectively) is expressed by

$$\langle p' | S_2 | p \rangle = i (2\pi)^4 \delta^{(4)}(p-p') \bar{u}_p(p) \Sigma_p(p) u_p(p). \quad (33)$$

It is straightforward but nevertheless cumbersome to calculate the proton mass function $\Sigma_p(x-y)$. One uses the explicit expression for the interpolating three-quark current given by Eq. (2) and the time-ordering of quark fields:

$$\langle 0 | T \{ q_f^\alpha(x) \bar{q}_{f'}^{\alpha'}(y) \} | 0 \rangle = \delta_{\alpha\alpha'} \delta_{ff'} S_f(x-y) = \delta_{\alpha\alpha'} \delta_{ff'} \int \frac{d^4 k}{(2\pi)^4 i} e^{-ik(x-y)} S_f(k), \quad (34)$$

where $S_f(x-y)$ and $S_f(k)$ are the free quark propagators in coordinate and momentum space with

$$S_f(k) = \frac{1}{m_f - \not{k}} \quad (35)$$

and where a, a' and f, f' are color and flavor indices, respectively.

In momentum space the proton mass function is given by

$$\Sigma_p(p) = 12g_N^2 \int \frac{d^4 k_1}{(2\pi)^4 i} \int \frac{d^4 k_2}{(2\pi)^4 i} \bar{\Phi}_N^2(-z_0) \Gamma^A \gamma^5 S_d(k_1 + w_1 p) \gamma^5 \Gamma^B \text{tr} [S_u(k_2 - w_2 p) \Gamma_A S_u(k_2 - k_1 + w_3 p) \Gamma_B] , \quad (36)$$

where

$$z_0 = \frac{1}{2}(k_1 - k_2)^2 + \frac{1}{6}(k_1 + k_2)^2. \quad (37)$$

In order to economize on the notation we introduce a short-hand notation for the two loop momentum integrations in (36) and in the following formulas. We write

$$\langle\langle \dots \rangle\rangle = \int \frac{d^4 k_1}{(2\pi)^4 i} \int \frac{d^4 k_2}{(2\pi)^4 i} (\dots). \quad (38)$$

Note that the integral Eq. (36) is invariant under a shift of the loop momenta $k_i \rightarrow k_i + ap$ where a is an arbitrary number and p is the outer momentum. Using this invariance one can obtain various equivalent representations for the mass function. In Eq. (36) we have chosen a such that the external momentum does not appear in the argument of the vertex function. One has $w_2 = w_3 = \frac{1}{2}(1 - w_1)$ where $w_1 = m_d/(m_d + 2m_u)$. We mention that it is convenient to keep $m_u \neq m_d$ in the analytical calculation in order to distinguish the proton from the neutron case. In the end, when we do the numerical calculation, we set $m_u = m_d$.

According to the compositeness condition Eq. (11) one needs to calculate the derivative of the proton mass function. Since the proton is on mass-shell, i.e. $\bar{u}(p) \not{p} u(p) = m_N \bar{u}(p) u(p)$ and hence $p^\mu \bar{u}(p) u(p) = m_N \bar{u}(p) \gamma^\mu u(p)$, the compositeness condition

$$\Sigma'_p(p) = \frac{\partial \Sigma_p(p)}{\partial \not{p}} = 1 \quad \text{with} \quad \not{p} = m_N \quad (39)$$

can be written as

$$\frac{\partial \Sigma_p(p)}{\partial p_\mu} = \gamma^\mu \quad \text{with} \quad \not{p} = m_N \quad \text{and} \quad p^\mu = m_N \gamma^\mu. \quad (40)$$

Here and in the following it is understood that the relations between Green functions are valid when sandwiched between spinors. The latter form (40) is more suitable for our calculation because of its relation to the electromagnetic proton vertex function at zero momentum transfer. Using

$$\frac{\partial}{\partial p_\mu} S_f(k + wp) = w S_f(k + wp) \gamma^\mu S_f(k + wp) \quad (41)$$

one obtains

$$\begin{aligned} \frac{\partial \Sigma_p(p)}{\partial p_\mu} = & 12g_N^2 \langle\langle \bar{\Phi}_N^2(-z_0) \left\{ w_1 \Gamma^A \gamma^5 S_d(k_1 + w_1 p) \gamma^\mu S_d(k_1 + w_1 p) \gamma^5 \Gamma^B \text{tr} [S_u(k_2 - w_2 p) \Gamma_A S_u(k_2 - k_1 + w_3 p) \Gamma_B] \right. \\ & - w_2 \Gamma^A \gamma^5 S_d(k_1 + w_1 p) \gamma^5 \Gamma^B \text{tr} [S_u(k_2 - w_2 p) \gamma^\mu S_u(k_2 - w_2 p) \Gamma_A S_u(k_2 - k_1 + w_3 p) \Gamma_B] \\ & \left. + w_3 \Gamma^A \gamma^5 S_d(k_1 + w_1 p) \gamma^5 \Gamma^B \text{tr} [S_u(k_2 - w_2 p) \Gamma_A S_u(k_2 - k_1 + w_3 p) \gamma^\mu S_u(k_2 - k_1 + w_3 p) \Gamma_B] \right\} \rangle\rangle. \quad (42) \end{aligned}$$

We now return to the calculation of the electromagnetic vertex of the proton. There are two terms in the relevant expansion of the S -matrix. These are derived i) from the Lagrangian Eq. (22) describing the local interaction of the photon with the quarks and ii) from the Lagrangian Eq. (27) describing the nonlocal interaction nucleon+quarks+photon. One has

$$\begin{aligned} S_3 = & i^3 g_N^2 \int dx \int dy \int dz A_\mu(z) \bar{p}(x) \langle 0 | T \{ J_p(x) (e_u \bar{u}(z) \gamma^\mu u(z) + e_d \bar{d}(z) \gamma^\mu d(z)) \bar{J}_p(y) \} | 0 \rangle p(y) \\ & + i^2 g_N^2 \int dx \int dy \int dz A_\mu(z) \bar{p}(x) \langle 0 | T \{ J_p(x) \bar{J}_{p-\text{em}}^\mu(y, z) + J_{p-\text{em}}^\mu(x, z) \bar{J}_p(y) \} | 0 \rangle p(y), \quad (43) \end{aligned}$$

where the currents $J_p(\bar{J}_p)$ and $J_{p-\text{em}}^\mu(\bar{J}_{p-\text{em}}^\mu)$ are defined by Eqs. (2) and (28), respectively. It is important to keep track of the signs of the various charges in the calculation. Our choice is to take the electric charges of charged particles in units of the proton charge, e.g. $e_p = +1$, $e_u = +2/3$, $e_d = -1/3$, etc.

The matrix element S_3 in Eq. (43) taken between the initial and final proton states with momenta (p) and (p') and the photon state with momentum ($q = p - p'$) reads

$$\langle p'; q, \mu | S_3 | p \rangle = \bar{u}_p(p') T_3^\mu(p; p', q) u_p(p). \quad (44)$$

The matrix element $T_3^\mu(p; p', q)$ is obtained from Eq. (43) by the substitutions $A_\mu(z) \rightarrow e^{iqz}$, $\bar{p}(x) \rightarrow e^{ip'x}$ and $p(y) \rightarrow e^{-ipy}$. A straightforward calculation gives

$$T_3^\mu(p; p', q) = i(2\pi)^4 \delta^{(4)}(p - p' - q) \Lambda_p^\mu(p, p') \quad (45)$$

where the electromagnetic vertex function $\Lambda_p^\mu(p, p')$ of the proton consists of four pieces represented by the four two-loop quark diagrams in Fig.2:

- the vertex diagram with the e.m. current attached to the d-quark (Fig.2a) — $\Lambda_{p\text{d}}^\mu$,
- the vertex diagram with the e.m. current attached to the u-quark (Fig.2b) — $\Lambda_{p\text{u}}^\mu$,
- two bubble diagrams with the e.m. current attached to the initial proton vertex (Fig.2c) — $\Lambda_{p(a)}^\mu$,
and with the e.m. current attached to the final proton vertex (Fig.2d) — $\Lambda_{p(b)}^\mu$.

The four different contributions can be calculated to be

$$\begin{aligned} \Lambda_{p\text{d}}^\mu(p, p') &= -4g_N^2 \left\langle \left\langle \bar{\Phi}_N(-z_0) \bar{\Phi}_N \left(-\frac{1}{2}(k_1 - k_2 + w_3q)^2 - \frac{1}{6}(k_1 + k_2 + (2w_2 + w_3)q)^2 \right) \right. \right. \\ &\quad \times \left. \Gamma^A \gamma^5 S_d(k_1 + w_1p') \gamma^\mu S_d(k_1 + w_1p' + q) \gamma^5 \Gamma^B \text{tr} [S_u(k_2 - w_2p') \Gamma_A S_u(k_2 - k_1 + w_3p') \Gamma_B] \right\rangle \right\rangle, \\ \Lambda_{p\text{u}}^\mu(p, p') &= 16g_N^2 \left\langle \left\langle \bar{\Phi}_N(-z_0) \bar{\Phi}_N \left(-\frac{1}{2}(k_1 - k_2 - (w_1 + w_2)q)^2 - \frac{1}{6}(k_1 + k_2 - (w_1 - w_2)q)^2 \right) \right. \right. \\ &\quad \times \left. \Gamma^A \gamma^5 S_d(k_1 + w_1p') \gamma^5 \Gamma^B \text{tr} [S_u(k_2 - w_2p') \Gamma_A S_u(k_2 - k_1 + w_3p') \gamma^\mu S_u(k_2 - k_1 + w_3p' + q) \Gamma_B] \right\rangle \right\rangle, \\ \Lambda_{p(a)}^\mu(p, p') &= 12g_N^2 \left\langle \left\langle \bar{\Phi}_N(-z_0) \tilde{E}_p^\mu(k_1 + w_1p', -k_2 + w_2p', k_2 - k_1 + w_3p'; q) \right. \right. \\ &\quad \times \left. \Gamma^A \gamma^5 S_d(k_1 + w_1p') \gamma^5 \Gamma^B \text{tr} [S_u(k_2 - w_2p') \Gamma_A S_u(k_2 - k_1 + w_3p') \Gamma_B] \right\rangle \right\rangle, \\ \Lambda_{p(b)}^\mu(p, p') &= 12g_N^2 \left\langle \left\langle \bar{\Phi}_N(-z_0) \tilde{E}_p^\mu(k_1 + w_1p, -k_2 + w_2p, k_2 - k_1 + w_3p; -q) \right. \right. \\ &\quad \times \left. \Gamma^A \gamma^5 S_d(k_1 + w_1p) \gamma^5 \Gamma^B \text{tr} [S_u(k_2 - w_2p) \Gamma_A S_u(k_2 - k_1 + w_3p) \Gamma_B] \right\rangle \right\rangle. \end{aligned} \quad (46)$$

The two bubble diagrams Figs. 2c-2d can be seen to be related by

$$\Lambda_{p(b)}^\mu(p, p') = \Lambda_{p(a)}^\mu(p', p). \quad (47)$$

Gauge invariance requires the validity of the $q^\mu = 0$ Ward identity

$$\frac{\partial \Sigma_p(p)}{\partial p_\mu} = \Lambda_p^\mu(p, p), \quad (48)$$

where $\Lambda_p^\mu(p, p)$ is given by the sum of the four contributions Eq. (46). The l.h.s. of (48) has been written down in Eq. (42). The contribution of the bubble diagrams to the r.h.s. of (48) is calculated by using the explicit representation of \tilde{E}_p^μ in Eq. (28). For the proton the quark charges are given by $e_1 = e_d$ and $e_2 = e_3 = e_u$. One finds

$$\begin{aligned} \Lambda_{p(a)}^\mu(p, p) + \Lambda_{p(b)}^\mu(p, p) &= 8(1 + 3w_1) g_N^2 \langle \langle k_1^\mu \bar{\Phi}'_N(-z_0) \bar{\Phi}_N(-z_0) \\ &\quad \times \Gamma^A \gamma^5 S_d(k_1 + w_1p) \gamma^5 \Gamma^B \text{tr} [S_u(k_2 - w_2p) \Gamma_A S_u(k_2 - k_1 + w_3p) \Gamma_B] \rangle \rangle. \end{aligned} \quad (49)$$

Superficially such terms are not present in Eq. (42) since (42) contains four quark propagators as a result of having differentiated the vertex function as compared to the three propagators in (49). However, the bubble contributions (49) may be rewritten in terms of the vertex diagram contributions at $q = 0$. This is achieved by using an integration-by-parts (IBP) identity where one differentiates the integrand w.r.t. the loop momentum k_1 . One has

$$\left\langle \left\langle \frac{\partial}{\partial k_1^\mu} \left\{ \bar{\Phi}_N^2(-z_0) \Gamma^A \gamma^5 S_d(k_1 + w_1 p) \gamma^5 \Gamma^B \text{tr} [S_u(k_2 - w_2 p) \Gamma_A S_u(k_2 - k_1 + w_3 p) \Gamma_B] \right\} \right\rangle \right\rangle \equiv 0. \quad (50)$$

Upon differentiation and use of the symmetry of the integrand under $k_2 \rightarrow -k_2 + k_1$ one obtains

$$\begin{aligned} & 2 \left\langle \left\langle k_1^\mu \bar{\Phi}'_N(-z_0) \bar{\Phi}_N(-z_0) \Gamma^A \gamma^5 S_d(k_1 + w_1 p) \gamma^5 \Gamma^B \text{tr} [S_u(k_2 - w_2 p) \Gamma_A S_u(k_2 - k_1 + w_3 p) \Gamma_B] \right\rangle \right\rangle \\ &= \left\langle \left\langle \bar{\Phi}_N^2(-z_0) \Gamma^A \gamma^5 S_d(k_1 + w_1 p) \gamma^\mu S_d(k_1 + w_1 p) \gamma^5 \Gamma^B \text{tr} [S_u(k_2 - w_2 p) \Gamma_A S_u(k_2 - k_1 + w_3 p) \Gamma_B] \right\rangle \right\rangle \\ &- \left\langle \left\langle \bar{\Phi}_N^2(-z_0) \Gamma^A \gamma^5 S_d(k_1 + w_1 p) \gamma^5 \Gamma^B \text{tr} [S_u(k_2 - w_2 p) \Gamma_A S_u(k_2 - k_1 + w_3 p) \gamma^\mu S_u(k_2 - k_1 + w_3 p) \Gamma_B] \right\rangle \right\rangle. \end{aligned} \quad (51)$$

Using the IBP-identity and summing up all contributions on the r.h.s. of Eq. (48) one finds agreement with the l.h.s. of Eq. (48) as given by Eq. (42). One has thus proven the validity of the Ward identity (48) (recall that $w_2 = w_3 = 1/2(1 - w_1)$).

A further technical remark is in order concerning the above check of the Ward identity Eq. (48). The proof made use of an IBP identity assuming the vanishing of the pertinent surface term. However, in the confinement ansatz with the accompanying IR cutoff the requisite surface terms no longer vanish. As it turns out one can avoid the use of IBP identities in the proof of the Ward identity by astutely shifting the loop momentum k_1 in the mass function. The appropriate shift is $k_1 \rightarrow k_1 + (w_2 + w_3 - \frac{4}{3})p$ and $k_2 \rightarrow k_2 + w_2 p$. One then obtains

$$\Sigma_p(p) = 12g_N^2 \int \frac{d^4 k_1}{(2\pi)^{4i}} \int \frac{d^4 k_2}{(2\pi)^{4i}} \bar{\Phi}_N^2(-z_1) \Gamma^A \gamma^5 S_d(k_1 - \frac{1}{3}p) \gamma^5 \Gamma^B \text{tr} [S_u(k_2) \Gamma_A S_u(k_2 - k_1 + \frac{4}{3}p) \Gamma_B], \quad (52)$$

where

$$z_1 = \frac{1}{2}(k_1 - k_2 + (w_3 - \frac{4}{3})p)^2 + \frac{1}{6}(k_1 + k_2 + (2w_2 + w_3 - \frac{4}{3})p)^2. \quad (53)$$

After the shift of the loop momentum the argument of the vertex function $\bar{\Phi}_N(-z_1)$ now depends on the external momentum p . When differentiating w.r.t. the external momentum p a new term will appear caused by the derivative of the vertex function $\bar{\Phi}_N$ in addition to the terms originating from the derivatives of the quark propagators. After shifting back the loop momenta $z_1 \rightarrow z_0$ and some algebraic juggling one finds that the derivative of the mass function coincides analytically with the expression for the electromagnetic vertex function $\Lambda_p^\mu(p, p)$ given by the sum of the contributions of the triangle diagrams (46) and the bubble diagrams Eq. (49). We emphasize that in this derivation we did not have to make use of an IBP identity to prove the Ward identity.

Hereafter we will use the compositeness condition $Z_N = 0$ in the form

$$\Lambda_{pd}^\mu(p, p) + \Lambda_{pu}^\mu(p, p) + \Lambda_{p(a)}^\mu(p, p) + \Lambda_{p(b)}^\mu(p, p) = \gamma^\mu \quad \text{with} \quad (\not{p} = m_N) \quad \text{and} \quad p^\mu = m_N \gamma^\mu \quad (54)$$

in order to determine the coupling constant g_N . This allows one to provide the correct normalization of the charged proton form factor within the confinement scenario.

Another useful check is to reproduce the generalized Ward-Takahashi identity

$$q_\mu \Lambda_p^\mu(p, p') = \Sigma_p(p) - \Sigma_p(p'). \quad (55)$$

We shall not elaborate on this proof which is straightforward by using suitable shifts of the loop variables.

Let us briefly describe another check on the gauge invariance of our calculation. Without gauge invariance there are three independent Lorentz structures in the electromagnetic proton vertex which can be chosen to be

$$\Lambda_p^\mu(p, p') = \gamma^\mu F_1^p(q^2) - \frac{i\sigma^{\mu q}}{2m_N} F_2^p(q^2) + q^\mu F_{NG}^p(q^2), \quad (56)$$

where $\sigma^{\mu q} = \frac{i}{2}(\gamma^\mu \gamma^\nu - \gamma^\nu \gamma^\mu) q_\nu$. The form factor $F_{NG}^p(q^2)$ characterizes the non-gauge invariant piece and must therefore vanish for any q^2 in a calculation which respects gauge invariance. For the four contributions of Fig. 2a-2d we found that

$$F_{NGd}^p(q^2) \equiv 0, \quad F_{NGu}^p(q^2) \equiv 0, \quad F_{NG(b)}^p(q^2) \equiv -F_{NG(a)}^p(q^2) \quad \forall q^2. \quad (57)$$

The gauge variant contributions of the two vertex diagrams are zero while they vanish for the sum of the two bubble diagrams.

Before discussing the e.m. properties of the neutron we would like to comment on a potential conflict between gauge invariance and our confinement ansatz. In general the IR cutoff used in Eq. (19) can destroy the gauge invariance as any cutoff can do. One can, however, show that in some special cases gauge invariance remains unimpaired when implementing confinement through an IR cutoff. For example, in Appendix B of [5] we have shown that the $\rho - \gamma$ transition amplitude is gauge invariant off mass-shell even in the presence of an IR cutoff. The crucial point of the proof was that we were able to show that the integrand of the t-integration itself was gauge invariant. In the case of the electromagnetic form factor of the proton one finds again that the integrand of the t-integration is gauge invariant by itself due to a symmetry property of the integrand in the space of the Schwinger α -parameters. However, if the proof of gauge invariance requires an integration by parts in the space of momenta which becomes translated into an integration by parts over the t-parameter gauge invariance will be spoiled by the surface term due to the upper integration limit $1/\lambda^2$. In order to keep gauge invariance one can proceed as follows. First, by using the properties of the relevant integrals over the loop momenta one needs to specify a gauge invariant part of the full amplitude. Then one employs our confinement ansatz for the gauge invariant parts of the amplitudes. Such an approach was used to verify the validity of the Ward identity when connecting the derivative of the mass function and the electromagnetic vertex function in the presence of an IR-cutoff.

The electromagnetic vertex function of the neutron is obtained from that of the proton by replacing $m_u \leftrightarrow m_d$, $e_u \leftrightarrow e_d$ and $m_p \rightarrow m_n$. $F_1^N(q^2)$ and $F_2^N(q^2)$ are the Dirac and Pauli nucleon form factors which are normalized to the electric charge e_N and anomalous magnetic moment k_N (k_N is given in units of the nuclear magneton $e/2m_p$), respectively, i.e. one has $F_1^N(0) = e_N$ and $F_2^N(0) = k_N$. In particular, one can analytically check by using the IBP identity that the Dirac form factor of the neutron is equal to zero at $q^2 = 0$.

The nucleon magnetic moments $\mu_N = F_1^N(0) + F_2^N(0)$ are known experimentally with high accuracy [20]

$$\mu_p^{\text{expt}} = 2.79 \quad \mu_n^{\text{expt}} = -1.91. \quad (58)$$

We will use these values to fit the value of the nucleon size parameter. The other model parameters are taken from the fit to mesonic transitions done in [6]:

m_u	m_s	m_c	m_b	λ	
0.235	0.424	2.16	5.09	0.181	GeV

(59)

We obtain

$$\text{vector current} \implies \Lambda_N = 0.36 \text{ GeV} \quad \mu_p = 2.79 \quad \mu_n = -1.70, \quad (60)$$

$$\text{tensor current} \implies \Lambda_N = 0.61 \text{ GeV} \quad \mu_p = 2.79 \quad \mu_n = -1.69. \quad (61)$$

It is convenient to introduce the Sachs electromagnetic form factors of nucleons

$$\begin{aligned} G_E^N(q^2) &= F_1^N(q^2) + \frac{q^2}{4m_N^2} F_2^N(q^2), \\ G_M^N(q^2) &= F_1^N(q^2) + F_2^N(q^2). \end{aligned} \quad (62)$$

The slopes of these form factors are related to the well-known electromagnetic radii of nucleons:

$$\langle r_E^2 \rangle^N = 6 \frac{dG_E^N(q^2)}{dq^2} \Big|_{q^2=0}, \quad (63)$$

$$\langle r_M^2 \rangle^N = \frac{6}{G_M^N(0)} \frac{dG_M^N(q^2)}{dq^2} \Big|_{q^2=0}. \quad (64)$$

We would like to emphasize that reproducing data on the neutron charge radius $\langle r_E^2 \rangle^n$ is a nontrivial task (see e.g. discussion in Ref.[10]). As well-known the naive nonrelativistic quark model based on SU(6) spin-flavor symmetry implies $\langle r_E^2 \rangle^n \equiv 0$. The dynamical breaking of the SU(6) symmetry based on the inclusion of the quark spin-spin interaction generates a nonvanishing value of $\langle r_E^2 \rangle^n$. From this point of view the dominant contribution to the $\langle r_E^2 \rangle^n$ comes from the Pauli term:

$$\langle r_E^2 \rangle^n \simeq \frac{6}{4m_N^2} F_2^n(0). \quad (65)$$

The experimental data on the nucleon Sachs form factors in the space-like region $Q^2 = -q^2 \geq 0$ can be approximately described by the dipole approximation

$$G_E^p(q^2) \approx \frac{G_M^p(q^2)}{1 + \mu_p} \approx \frac{G_M^n(q^2)}{\mu_n} \approx \frac{4m_N^2 G_E^n(q^2)}{q^2 \mu_n} \approx \frac{1}{(1 - q^2/0.71 \text{ GeV}^2)^2} \equiv D_N(q^2). \quad (66)$$

According to present data the dipole approximation works well up to 1 GeV^2 (with an accuracy of up to 25%). For higher values of Q^2 the deviation of the nucleon form factors from the dipole approximation becomes more pronounced. In particular, the best description of magnetic moments, electromagnetic radii and form factors is achieved when we consider a superposition of the V - and T -currents of nucleons according to Eq. (3) with $x = 0.8$. For the size parameter of the nucleon we take $\Lambda_N = 0.5 \text{ GeV}$.

In Table I we present the results for the magnetic moments and electromagnetic radii for this set of model parameters. In Fig. 3 we present our results for the q^2 dependence of electromagnetic form factors in the region $Q^2 \in [0, 1] \text{ GeV}^2$. Fig. 3 also shows plots of the dipole approximation to the form factors. The agreement of our results with the dipole approximation is satisfactory. Inclusion of chiral corrections as, for example, developed and discussed in [21] may lead to a further improvement in the low Q^2 description.

V. Λ -TYPE MASS FUNCTION AND ELECTROMAGNETIC VERTEX

In a future publication we plan to study the rare baryon decays $\Lambda_b \rightarrow \Lambda_s \ell^+ \ell^-$ in the context of the covariant quark model [9]. It is the purpose of this section to provide the necessary material that allows for a covariant quark model description of the $\Lambda = (Q[ud])$ -type baryons composed of a (s, c, b) quark Q and a light diquark-like state $[ud]$ with spin and isospin zero.

In general, for the Λ -type baryons one can construct three types of currents without derivatives — pseudoscalar J^P , scalar J^S and axial-vector J^A (see, Refs. [1, 4, 22, 23]):

$$\begin{aligned} J_{\Lambda_{Q[ud]}}^P &= \epsilon^{a_1 a_2 a_3} Q^{a_1} u^{a_2} C \gamma_5 d^{a_3}, \\ J_{\Lambda_{Q[ud]}}^S &= \epsilon^{a_1 a_2 a_3} \gamma^5 Q^{a_1} u^{a_2} C d^{a_3}, \\ J_{\Lambda_{Q[ud]}}^A &= \epsilon^{a_1 a_2 a_3} \gamma^\mu Q^{a_1} u^{a_2} C \gamma_5 \gamma_\mu d^{a_3}. \end{aligned} \quad (67)$$

There are only two independent linear combinations of the above three currents given by $J^V = (2J^P - 2J^S + J^A)/3$ and $J^T = J^P + J^S$. The symbol $[ud]$ denotes antisymmetrization of both flavor and spin indices w.r.t. the light quarks u and d . We will consider three flavor types of the Λ -baryons: $\Lambda_s^0[ud]$, $\Lambda_c^+[ud]$ and $\Lambda_b^0[ud]$. In Ref. [3] we have shown that, in the nonrelativistic limit, the J^P and J^A interpolating currents of the $\Lambda_{Q[ud]}$ baryons become degenerate and attain the (same) correct nonrelativistic limit (in the case of single-heavy baryons this limit coincides with the heavy quark limit), while the J^S current vanishes in the nonrelativistic limit. On the other hand, the J^P and J^A interpolating currents of Λ -type baryons become degenerate with their $\text{SU}(N_f)$ -symmetric currents in the nonrelativistic limit. In Ref. [22] we have shown that in case of the heavy-to-light baryon transition $\Lambda_c^+ \rightarrow \Lambda^0 e^+ \nu_e$ the use of a $\text{SU}(3)$ symmetric current for the Λ^0 hyperon is essential in order to describe data on $\Gamma(\Lambda_c^+ \rightarrow \Lambda^0 e^+ \nu_e)$ (see also discussion in Refs. [24, 25]). Therefore, in the following we restrict ourselves to the simplest pseudoscalar J^P current. The nonlocal interpolating three-quark current is written as

$$\begin{aligned} J_\Lambda(x) &= \int dx_1 \int dx_2 \int dx_3 F_\Lambda(x; x_1, x_2, x_3) J_{3q}^{(\Lambda)}(x_1, x_2, x_3), \\ J_{3q}^{(\Lambda)}(x_1, x_2, x_3) &= \frac{1}{2} \epsilon^{a_1 a_2 a_3} Q_{a_1}(x_1) (u^{a_2}(x_2) C \gamma^5 d^{a_3}(x_3) - d^{a_2}(x_3) C \gamma^5 u^{a_3}(x_2)) \\ &= \epsilon^{a_1 a_2 a_3} Q^{a_1}(x_1) u^{a_2}(x_2) C \gamma^5 d^{a_3}(x_3), \\ \bar{J}_\Lambda(x) &= \int dx_1 \int dx_2 \int dx_3 F_\Lambda(x; x_1, x_2, x_3) \bar{J}_{3q}^{(\Lambda)}(x_1, x_2, x_3), \\ \bar{J}_{3q}^{(\Lambda)}(x_1, x_2, x_3) &= \epsilon^{a_1 a_2 a_3} \bar{d}^{a_3}(x_3) \gamma^5 C \bar{u}^{a_2}(x_2) \cdot \bar{Q}^{a_1}(x_1), \end{aligned} \quad (68)$$

where $Q = s, c, b$.

The calculation of the Λ -type mass function and the electromagnetic vertex proceeds in the same way as in the nucleon case. The matrix elements in momentum space read

$$\Sigma_\Lambda(p) = 6g_\Lambda^2 \left\langle \left\langle \bar{\Phi}_\Lambda^2(-z_0) S_Q(k_1 + w_1 p) \text{tr} [S_u(k_2 - w_2 p) \gamma^5 S_d(k_2 - k_1 + w_3 p) \gamma^5] \right\rangle \right\rangle, \quad (69)$$

where we use the same short-hand notation $\langle\langle \dots \rangle\rangle$ for the two-fold loop-momentum integration as before (see Eqs. (38)). The variable z_0 is defined in (37).

The various contributions to the electromagnetic vertex are given by

$$\begin{aligned}
\Lambda_{\Lambda_Q}^\mu(p, p') &= 6 e_Q g_\Lambda^2 \langle\langle \bar{\Phi}_\Lambda(-z_0) \bar{\Phi}_\Lambda \left(-\frac{1}{2}(k_1 - k_2 + w_3 q)^2 - \frac{1}{6}(k_1 + k_2 + (2w_2 + w_3)q)^2 \right) \\
&\quad \times S_Q(k_1 + w_1 p') \gamma^\mu S_Q(k_1 + w_1 p' + q) \text{tr} [S_u(k_2 - w_2 p') \gamma^5 S_d(k_2 - k_1 + w_3 p') \gamma^5] \rangle\rangle, \\
\Lambda_{\Lambda_u}^\mu(p, p') &= -6 e_u g_\Lambda^2 \langle\langle \bar{\Phi}_\Lambda(-z_0) \bar{\Phi}_\Lambda \left(-\frac{1}{2}(k_1 - k_2 + w_3 q)^2 - \frac{1}{6}(k_1 + k_2 - (2w_1 + w_3)q)^2 \right) \\
&\quad \times S_Q(k_1 + w_1 p') \text{tr} [S_u(k_2 - w_2 p' - q) \gamma^\mu S_u(k_2 - w_2 p') \gamma^5 S_d(k_2 - k_1 + w_3 p') \gamma^5] \rangle\rangle, \\
\Lambda_{\Lambda_d}^\mu(p, p') &= 6 e_d g_\Lambda^2 \langle\langle \bar{\Phi}_\Lambda(-z_0) \bar{\Phi}_\Lambda \left(-\frac{1}{2}(k_1 - k_2 - (w_1 + w_2)q)^2 - \frac{1}{6}(k_1 + k_2 - (w_1 - w_2)q)^2 \right) \\
&\quad \times S_Q(k_1 + w_1 p') \text{tr} [S_u(k_2 - w_2 p') \gamma^5 S_d(k_2 - k_1 + w_3 p') \gamma^\mu S_d(k_2 - k_1 + w_3 p' + q) \gamma^5] \rangle\rangle, \\
\Lambda_{\Lambda^{(a)}}^\mu(p, p') &= 6 g_\Lambda^2 \langle\langle \bar{\Phi}_\Lambda(-z_0) \tilde{E}_\Lambda^\mu(k_1 + w_1 p', -k_2 + w_2 p', k_2 - k_1 + w_3 p'; q) \\
&\quad \times S_Q(k_1 + w_1 p') \text{tr} [S_u(k_2 - w_2 p') \gamma^5 S_d(k_2 - k_1 + w_3 p') \gamma^5] \rangle\rangle, \\
\Lambda_{\Lambda^{(b)}}^\mu(p, p') &= 6 g_\Lambda^2 \langle\langle \bar{\Phi}_\Lambda(-z_0) \tilde{E}_\Lambda^\mu(k_1 + w_1 p, -k_2 + w_2 p, k_2 - k_1 + w_3 p; -q) \\
&\quad \times S_Q(k_1 + w_1 p) \text{tr} [S_u(k_2 - w_2 p) \gamma^5 S_d(k_2 - k_1 + w_3 p) \gamma^5] \rangle\rangle. \tag{70}
\end{aligned}$$

One now has three e.m. vertex contributions because there are three different quarks in the Λ_Q state. The function $\tilde{E}_\Lambda^\mu(r_1, r_2, r_3; r)$ has been defined in Eq. (28). The variables $q_1 = \sum_{i=1}^3 w_{i1} r_i$ and $q_2 = \sum_{i=1}^3 w_{i2} r_i$ in $\tilde{E}_\Lambda^\mu(r_1, r_2, r_3; r)$ can be seen to be related to the loop momenta by

$$q_1 = \frac{1}{\sqrt{2}}(k_1 - k_2), \quad q_2 = -\frac{1}{\sqrt{6}}(k_1 + k_2) \tag{71}$$

for both bubble diagrams. By using Eq. (71) one finds the $q = 0$ relations

$$\begin{aligned}
\Lambda_{\Lambda^{(a)}}^\mu(p, p) + \Lambda_{\Lambda^{(b)}}^\mu(p, p) &= -8 g_\Lambda^2 \langle\langle (Q_1 k_1^\mu + Q_2 k_2^\mu) \bar{\Phi}'_\Lambda(-z_0) \bar{\Phi}_\Lambda(-z_0) \\
&\quad \times S_Q(k_1 + w_1 p) \text{tr} [S_u(k_2 - w_2 p) \gamma^5 S_d(k_2 - k_1 + w_3 p) \gamma^5] \rangle\rangle, \\
Q_1 &= e_1(w_2 + 2w_3) - e_2(w_1 - w_3) - e_3(2w_1 + w_2), \\
Q_2 &= e_1(w_2 - w_3) - e_2(w_1 + 2w_3) + e_3(w_1 + 2w_2). \tag{72}
\end{aligned}$$

where the subscripts on the charges e_i refer to the flavors of the three quarks: " $i = 1$ " \rightarrow " s, c, b ", " $i = 2$ " \rightarrow " u " and " $i = 3$ " \rightarrow " d ". Next we will use an IBP-identity to write

$$\left\langle\left\langle \frac{\partial}{\partial k_i^\mu} \left\{ \bar{\Phi}_\Lambda^2(-z_0) S_Q(k_1 + w_1 p) \text{tr} [S_u(k_2 - w_2 p) \gamma^5 S_d(k_2 - k_1 + w_3 p) \gamma^5] \right\} \right\rangle\right\rangle \equiv 0, \quad (i = 1, 2). \tag{73}$$

One finds

$$\begin{aligned}
\langle\langle k_1^\mu A_0 \rangle\rangle &= \frac{1}{4} \langle\langle (2A_1^\mu + A_2^\mu - A_3^\mu) \rangle\rangle, \\
\langle\langle k_2^\mu A_0 \rangle\rangle &= \frac{1}{4} \langle\langle (A_1^\mu + 2A_2^\mu + A_3^\mu) \rangle\rangle, \tag{74}
\end{aligned}$$

where

$$\begin{aligned}
A_0 &= \bar{\Phi}'_\Lambda(-z_0) \bar{\Phi}_\Lambda(-z_0) S_Q(k_1 + w_1 p) \text{tr} [S_u(k_2 - w_2 p) \gamma^5 S_d(k_2 - k_1 + w_3 p) \gamma^5], \\
A_1^\mu &= \bar{\Phi}_\Lambda^2(-z_0) S_Q(k_1 + w_1 p) \gamma^\mu S_Q(k_1 + w_1 p) \text{tr} [S_u(k_2 - w_2 p) \gamma^5 S_d(k_2 - k_1 + w_3 p) \gamma^5], \\
A_2^\mu &= \bar{\Phi}_\Lambda^2(-z_0) S_Q(k_1 + w_1 p) \text{tr} [S_u(k_2 - w_2 p) \gamma^\mu S_u(k_2 - w_2 p) \gamma^5 S_d(k_2 - k_1 + w_3 p) \gamma^5], \\
A_3^\mu &= \bar{\Phi}_\Lambda^2(-z_0) S_Q(k_1 + w_1 p) \text{tr} [S_u(k_2 - w_2 p) \gamma^5 S_d(k_2 - k_1 + w_3 p) \gamma^\mu S_d(k_2 - k_1 + w_3 p) \gamma^5]. \tag{75}
\end{aligned}$$

Using these identities and collecting all pieces together, one has

$$\Lambda_{\Lambda}^{\mu}(p, p) = (e_Q + e_u + e_d) \frac{\partial \Sigma_{\Lambda}(p)}{\partial p^{\mu}}, \quad \not{p} = m_{\Lambda}. \quad (76)$$

As was discussed above, this Ward identity allows one to use the compositeness condition $Z_{\Lambda} = 0$ written in the form

$$\Lambda_{\Lambda}^{\mu}(p, p) = \gamma^{\mu}, \quad \not{p} = m_{\Lambda}, \quad (77)$$

where we take $e_Q = e_c$ for the present discussion. Again we have checked analytically that, on the Λ -type baryon mass shell, the vertex diagrams are gauge invariant by themselves and the non-gauge invariant parts coming from the bubble diagrams corresponding to Fig.2(c) and 2(d) cancel each other before t -integration. The standard definition of the electromagnetic form factors is

$$\Lambda_{\Lambda}^{\mu}(p, p') = \gamma_{\mu} F_1(q^2) - \frac{i\sigma^{\mu q}}{2m_{\Lambda}} F_2(q^2), \quad (78)$$

where $\sigma^{\mu q} = \frac{i}{2}(\gamma^{\mu}\gamma^{\nu} - \gamma^{\nu}\gamma^{\mu})q_{\nu}$. The magnetic moment of the Λ -type baryon is defined by

$$\mu_{\Lambda} = (F_1(0) + F_2(0)) \frac{e}{2m_{\Lambda}}. \quad (79)$$

In terms of the nuclear magneton (n.m.) $\frac{e}{2m_p}$ the Λ -type baryon magnetic moment the Λ -hyperon magnetic moment is given by

$$\mu_{\Lambda} = (F_1(0) + F_2(0)) \frac{m_p}{m_{\Lambda}}, \quad (80)$$

where m_p is the proton mass.

In the present paper we shall only make a rather cursory investigation into the possible values of the size parameters of the $\Lambda = (Q[ud])$ -type baryons. A more detailed investigation will be left to our future publication [9] where we will include information on the charged current transitions $\Lambda_b \rightarrow \Lambda_c$ and $\Lambda_c \rightarrow \Lambda_s$ to specify the values of the size parameters of the $\Lambda = (Q[ud])$ -type baryons.

Let us assume for the moment that the size parameters are the same for all Λ -type baryons. One then has

$$\begin{aligned} \Lambda_{\Lambda} &= 0.5 \text{ GeV} & \mu_{\Lambda_s} &= -0.73, & \mu_{\Lambda_c} &= +0.36, & \mu_{\Lambda_b} &= -0.06, \\ \Lambda_{\Lambda} &= 1.0 \text{ GeV} & \mu_{\Lambda_s} &= -0.68, & \mu_{\Lambda_c} &= +0.40, & \mu_{\Lambda_b} &= -0.06, \\ \Lambda_{\Lambda} &= 1.5 \text{ GeV} & \mu_{\Lambda_s} &= -0.61, & \mu_{\Lambda_c} &= +0.44, & \mu_{\Lambda_b} &= -0.07. \end{aligned} \quad (81)$$

The magnetic moment of the Λ_s has to be compared with the experimental value listed in [20]

$$\mu_{\Lambda_s} = -0.613 \pm 0.004. \quad (82)$$

Eq. (81) shows that the value of the magnetic moment of the Λ_s is quite stable against variations of its size parameter. There is no experimental information on the magnetic moments of the Λ_b and Λ_c .

The calculation of the form factors in our approach is automated by the use of FORM and FORTRAN packages written for this purpose. In order to be able to compare with our earlier unconfined calculations we have written two versions for the confined and the unconfined versions of the covariant quark model.

VI. SUMMARY AND CONCLUSIONS

We have extended our previous formulation of the confined covariant quark model for mesons and tetraquark states to the baryon sector. We have discussed in some detail various calculational aspects of the two-loop baryon problem such as the evaluation of the baryon mass operator and its derivative, the implementation of confinement in the two-loop context, the calculation of electromagnetic current-induced transition matrix elements and the analytical verification of the pertinent Ward and Ward–Takahashi identities associated with the electromagnetic matrix elements.

In our numerical work we have used the same values of the constituent quark masses and infrared cutoff as had been obtained before in the meson sector by a fit to various mesonic transition matrix elements. In this way the number of model parameters were kept to a minimum.

Using two parameters we have calculated the nucleon magnetic moments and charge radii as well as the electromagnetic form factors at low momentum transfers. An extension of our work to the $N - \Delta(1236)$ transition can be done along the lines described in [26].

We have also discussed light and heavy $\Lambda = (Q[ud])$ -type baryons. In particular we obtained a value for the size parameter of the Λ_s by a fit to its experimentally known magnetic moment. By determining the properties of the $\Lambda = (Q[ud])$ -type baryons we have laid the groundwork for a calculation of the rare decays of the Λ_b -baryon (such as $\Lambda_b \rightarrow \Lambda_s \ell^+ \ell^-$) within the framework of the covariant quark model.

Acknowledgments

This work was supported by the DFG under Contract No. LY 114/2-1, by the Federal Targeted Program “Scientific and scientific-pedagogical personnel of innovative Russia” Contract No.02.740.11.0238. M.A.I. acknowledges the support of the Forschungszentrum of the Johannes Gutenberg–Universität Mainz “Elementarkräfte und Mathematische Grundlagen (EMG)” and Russian Fund of Basic Research grant No. 10-02-00368-a.

-
- [1] A. Faessler, T. Gutsche, M. A. Ivanov, J. G. Körner and V. E. Lyubovitskij, Phys. Lett. B **518** (2001) 55 [hep-ph/0107205].
- [2] A. Faessler, T. Gutsche, B. R. Holstein, M. A. Ivanov, J. G. Körner and V. E. Lyubovitskij, Phys. Rev. D **78** (2008) 094005 [arXiv:0809.4159 [hep-ph]].
- [3] A. Faessler, T. Gutsche, M. A. Ivanov, J. G. Körner and V. E. Lyubovitskij, Phys. Rev. D **80** (2009) 034025 [arXiv:0907.0563 [hep-ph]].
- [4] T. Branz, A. Faessler, T. Gutsche, M. A. Ivanov, J. G. Körner, V. E. Lyubovitskij and B. Oexl, Phys. Rev. D **81** (2010) 114036 [arXiv:1005.1850 [hep-ph]].
- [5] T. Branz, A. Faessler, T. Gutsche, M. A. Ivanov, J. G. Körner and V. E. Lyubovitskij, Phys. Rev. D **81** (2010) 034010 [arXiv:0912.3710 [hep-ph]].
- [6] M. A. Ivanov, J. G. Körner, S. G. Kovalenko, P. Santorelli and G. G. Saidullaeva, Phys. Rev. D **85**, 034004 (2012) [arXiv:1112.3536 [hep-ph]].
- [7] S. Dubnicka, A. Z. Dubnickova, M. A. Ivanov, J. G. Körner, Phys. Rev. **D81**, 114007 (2010). [arXiv:1004.1291 [hep-ph]]; S. Dubnicka, A. Z. Dubnickova, M. A. Ivanov, J. G. Körner and G. G. Saidullaeva, AIP Conf. Proc. **1343**, 385 (2011) [arXiv:1011.4417 [hep-ph]].
- [8] S. Dubnicka, A. Z. Dubnickova, M. A. Ivanov, J. G. Körner, P. Santorelli and G. G. Saidullaeva, Phys. Rev. D **84**, 014006 (2011) [arXiv:1104.3974 [hep-ph]].
- [9] T. Gutsche, M. A. Ivanov, J. G. Körner, V. E. Lyubovitskij and P. Santorelli, in preparation.
- [10] W. R. B. de Araujo, T. Frederico, M. Beyer and H. J. Weber, Int. J. Mod. Phys. A **18**, 5767 (2003) [hep-ph/0305120].
- [11] M. A. Ivanov, M. P. Locher and V. E. Lyubovitskij, Few Body Syst. **21** (1996) 131.
- [12] S. Weinberg, Phys. Rev. **130**, 776 (1963).
- [13] A. Salam, Nuovo Cim. **25**, 224 (1962).
- [14] K. Hayashi, M. Hirayama, T. Muta, N. Seto and T. Shirafuji, Fortsch. Phys. **15**, 625 (1967).
- [15] G. V. Efimov and M. A. Ivanov, *The Quark Confinement Model of Hadrons*, (IOP Publishing, Bristol & Philadelphia, 1993).
- [16] J. A. M. Vermaseren, Nucl. Phys. Proc. Suppl. **183**, 19 (2008) [arXiv:0806.4080 [hep-ph]]; arXiv:math-ph/0010025. S. Dubnicka, A. Z. Dubnickova, M. A. Ivanov and J. G. Körner, Phys. Rev. D **81**, 114007 (2010) [arXiv:1004.1291 [hep-ph]].
- [17] S. Mandelstam, Annals Phys. **19**, 1 (1962).
- [18] J. Terning, Phys. Rev. D **44**, 887 (1991).
- [19] A. Faessler, T. Gutsche, M. A. Ivanov, J. G. Körner, V. E. Lyubovitskij, D. Nicmorus and K. Pumsa-ard, Phys. Rev. D **73**, 094013 (2006) [hep-ph/0602193].
- [20] K. Nakamura *et al.* [Particle Data Group Collaboration], J. Phys. G **G37** (2010) 075021.
- [21] A. Faessler, T. Gutsche, V. E. Lyubovitskij and K. Pumsa-ard, Phys. Rev. D **73** (2006) 114021 [hep-ph/0511319].
- [22] M. A. Ivanov, V. E. Lyubovitskij, J. G. Körner and P. Kroll, Phys. Rev. D **56**, 348 (1997) [arXiv:hep-ph/9612463].
- [23] M. A. Ivanov, J. G. Körner, V. E. Lyubovitskij and A. G. Rusetsky, Phys. Lett. B **476**, 58 (2000) [arXiv:hep-ph/9910342].
- [24] J. G. Körner, M. Krämer and D. Pirjol, Prog. Part. Nucl. Phys. **33**, 787 (1994) [hep-ph/9406359].
- [25] H. -Y. Cheng and B. Tseng, Phys. Rev. D **53** (1996) 1457 [Erratum-ibid. D **55** (1997) 1697] [hep-ph/9502391].
- [26] A. Faessler, T. Gutsche, B. R. Holstein, V. E. Lyubovitskij, D. Nicmorus and K. Pumsa-ard, Phys. Rev. D **74**, 074010 (2006) [hep-ph/0608015].

TABLE I: Electromagnetic properties of nucleons

Quantity	Our results	Data [20]
μ_p (in n.m.)	2.96	2.793
μ_n (in n.m.)	-1.83	-1.913
r_E^p (fm)	0.805	0.8768 ± 0.0069
$\langle r_E^2 \rangle^n$ (fm ²)	-0.121	-0.1161 ± 0.0022
r_M^p (fm)	0.688	$0.777 \pm 0.013 \pm 0.010$
r_M^n (fm)	0.685	$0.862^{+0.009}_{-0.008}$

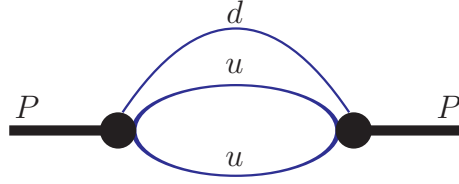


FIG. 1: Proton mass operator.

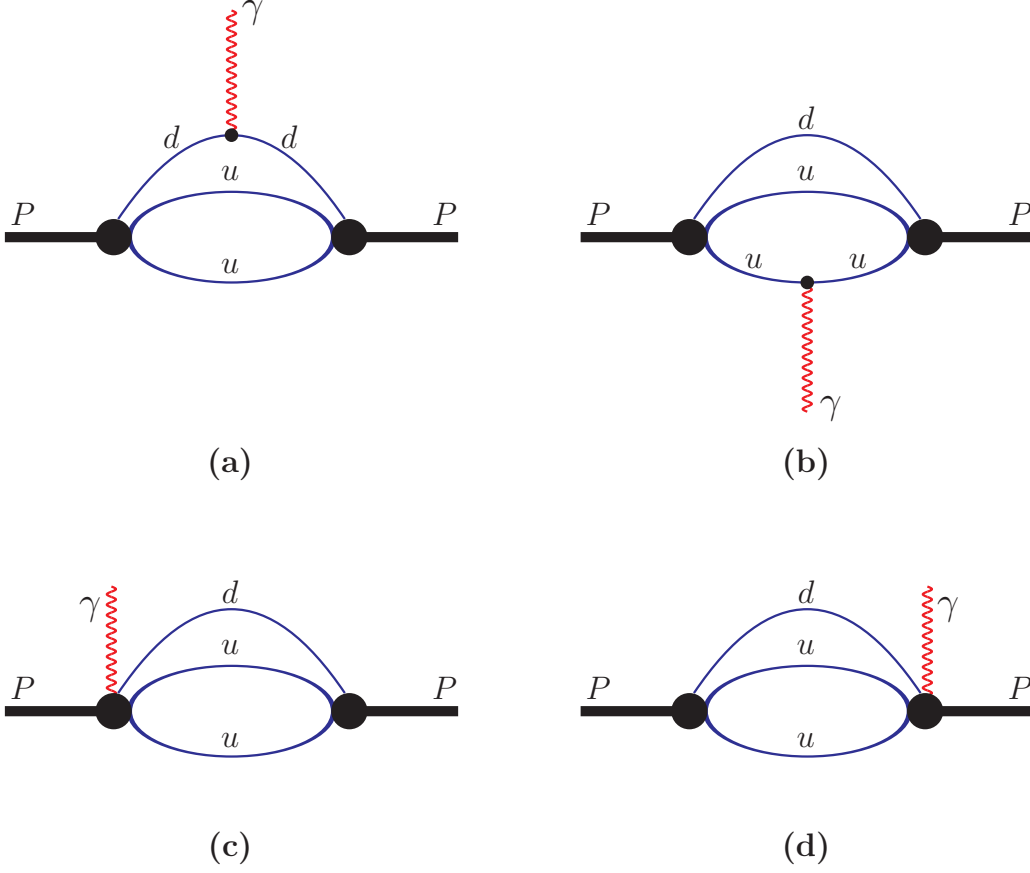


FIG. 2: Electromagnetic vertex function of the proton: (a) vertex diagram with the e.m. current attached to d-quark; (b) vertex diagram with the e.m. current attached to u-quark; (c) bubble diagram with the e.m. current attached to the initial state vertex; (d) the bubble diagram with e.m. current attached to the final state vertex.

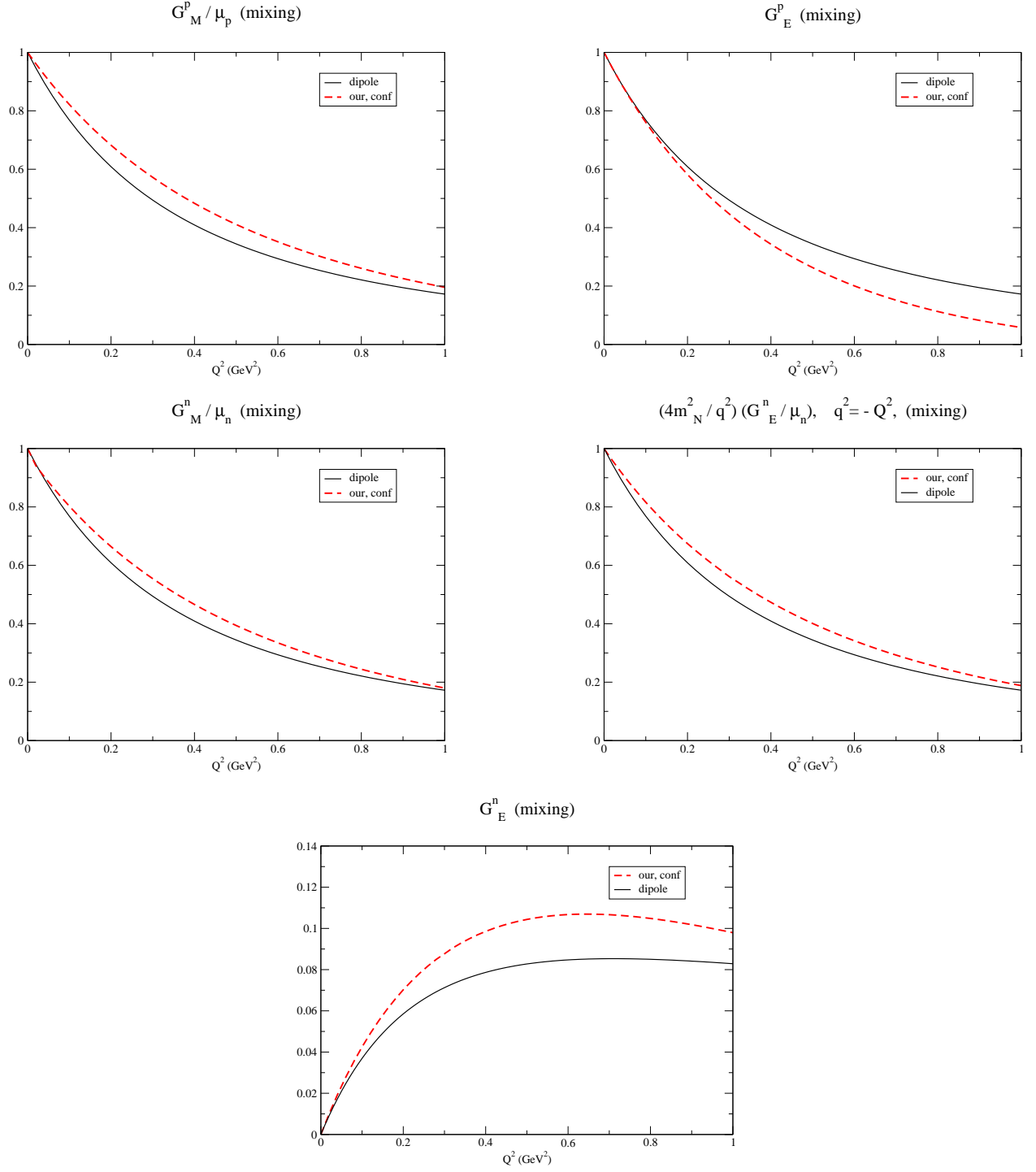


FIG. 3: Sachs nucleon form factors in comparisons with the dipole representation in the space-like region $Q \leq 1$ GeV².